Reactions of pulsed laser produced boron and nitrogen atoms in a condensing argon stream

Lester Andrews, Parviz Hassanzadeh, Thomas R. Burkholder, and J. M. L. Martin

Citation: The Journal of Chemical Physics **98**, 922 (1993); doi: 10.1063/1.464256
View online: http://dx.doi.org/10.1063/1.464256
View Table of Contents: http://scitation.aip.org/content/aip/journal/jcp/98/2?ver=pdfcov
Published by the AIP Publishing

Reactions of pulsed laser produced boron and nitrogen atoms in a condensing argon stream

Lester Andrews, Parviz Hassanzadeh, and Thomas R. Burkholder
Department of Chemistry, University of Virginia, Charlottesville, Virginia 22901

J. M. L. Martin[a)]
San Diego Supercomputer Center, San Diego, California 92186

(Received 3 August 1992; accepted 8 October 1992)

Reactions of pulsed laser produced B and N atoms at high dilution in argon favored diboron species. At low laser power with minimum radiation, the dominant reaction with N_2 gave BBNN ($^3\Pi$). At higher laser power, reactions of N atoms contributed the B_2N ($^2B_2$), BNB ($^2\Sigma_u^+$), NNBN ($^1\Sigma^+$), and BNBN ($^3\Pi$) species. These new transient molecules were identified from mixed isotopic patterns, isotopic shifts, and *ab initio* calculations of isotopic spectra.

I. INTRODUCTION

Solid boron nitride (BN) is a refractory material with many applications. The molecular B_xN_y vapor species are important because thin films of boron nitride can be grown by vapor deposition for high-temperature coatings.[1] A convenient way to produce vapors of refractory materials is by pulsed laser vaporization. The vapors so formed have been examined by mass spectroscopy[2,3] and by matrix electron spin resonance (ESR) spectroscopy.[4] The major species characterized by ESR is the linear $^2\Sigma_u^+$ BNB radical. Detailed *ab initio* studies of possible binary vapor species in the BN system have also been presented.[5]

Pulsed laser evaporation for matrix infrared studies of small molecules has been applied in this laboratory to phosphorous, boron, and aluminum oxides.[6–8] Boron nitride was explored as a possible source of boron atoms for argon matrix reactions; instead intense new infrared absorptions, with boron isotopic multiplets, were observed. These B_xN_y vapor species were also prepared by boron–nitrogen reactions in excess argon, which will be characterized here.

II. EXPERIMENT

A closed-cycle helium refrigerator (CTI Cryogenics Model 22) supported in a custom-designed stainless-steel chamber was used to cool (12±1 K) a copper block containing a CsI window. The pulsed YAG laser evaporation experiment employed here has been described previously[7,9] and is similar to the technique employed by Knight and co-workers.[4] Pieces of solid boron nitride (Johnson Mathey/Aesar and Carborundum) were affixed to a rod and rotated at 1 r.p.m., and boron nitride was evaporated directly into an argon stream by a focused YAG laser (10–60 mJ/pulse at the sample). Complementary experiments were done by codepositing pulsed laser evaporated B atoms with Ar/N_2 samples. Natural and enriched isotopic nitrogen (Isomet and Cambridge Isotope Laboratories) and isotopic boron samples (Eagle-Pitcher Industries) were employed. Infrared spectra were recorded on a Nicolet 5DXB at 2 cm^{-1} and a Nicolet 60SXR at 0.5 cm^{-1} resolution. Samples were also subjected to annealing and medium pressure mercury arc photolysis.

III. RESULTS

Infrared spectra of boron nitride ablation products and boron-atom–nitrogen-atom and molecule reaction products in solid argon will be presented.

A. Boron nitride

Boron nitride is hydroscopic and slowly hydrolyzes to NH_3, B_2O_3, and further to $B(OH)_3$. Infrared absorptions for B_2O_3, $B(OH)_3$, BO, BO_2, BOB, HBO, BO_2^-, and B_2O_2 were observed in all of these experiments.[7,10,11] These impurity absorptions were minimized to trace levels after preparing a fresh BN surface and immediately putting the BN target under vacuum. Boron nitride ablation targets were used for a total of fifteen infrared matrix isolation experiments. All were characterized by a very strong boron isotopic triplet absorption at 901.6, 891.1, and 882.3 cm^{-1} with 1/8/16 relative intensities. These bands were sharper at lower laser power and such a spectrum is illustrated in Fig. 1(a) for a 1.5 h codeposition with argon on a 12±1 K substrate. Further sample deposition increased the band absorbances and broadened the bands particularly in the higher wave-number region.

Additional weaker absorptions observed in the 2100–1700 cm^{-1} region, shown in Fig. 1, are also of interest here. A weak 1/8/16 triplet at 1769.2, 1753.5, and 1736.5 cm^{-1} (labeled *B*) decreased on photolysis and on annealing. New bands were observed at 1802.2 cm^{-1} (labeled *C*), 1912.5 cm^{-1} (labeled *D*), 1958.7 cm^{-1} (labeled *E*), 1998.4 cm^{-1} (labeled *A*), and 2091.8 cm^{-1} (labeled *C*) as listed in Table I.

The strong triplet (labeled *A*) was accompanied by a series of combination bands also illustrated in Fig. 1(a) and listed in Table II. The combination bands are associated with species *A* by common boron isotopic splittings, matrix site patterns, and annealing behavior. Furthermore, the same *A* bands were produced at lower yield by the

[a)]On leave from Limburgs Universitair Centrum, Department SBG, Universitaire Campus, B-3590 Diepenbeek, Belgium, and University of Antwerp (UIA), Department of Chemistry, Institute for Materials Science, Universiteitsplein 1, B-2610 Wilrijk, Belgium.

 0021-9606/93/020922-10$06.00

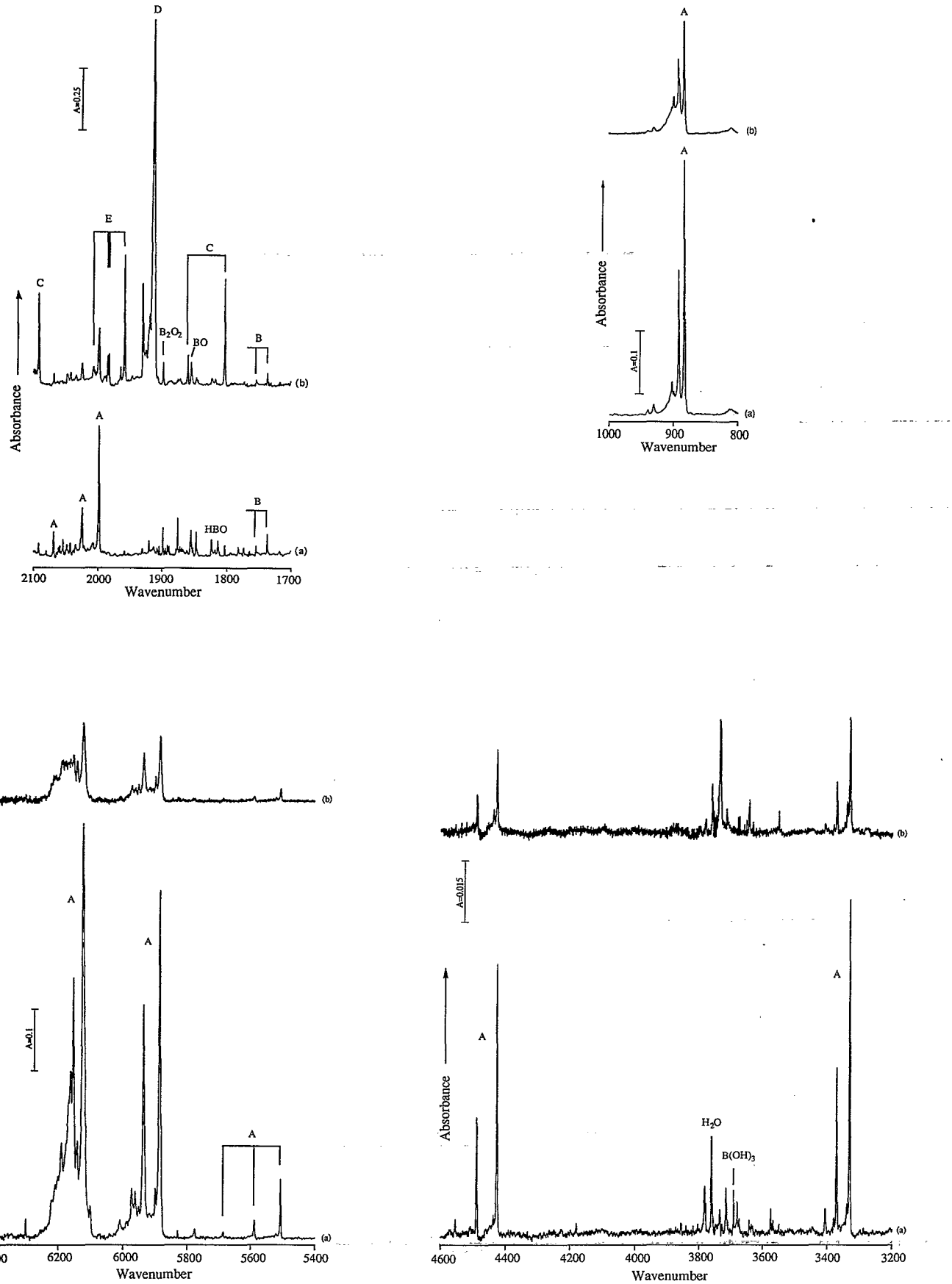

FIG. 1. Infrared spectra of boron–nitrogen samples in four spectral regions. (a) Boron–nitride sample laser ablated by 20 mJ/pulse at the sample into a condensing argon stream for 1.5 h; (b) natural isotopic boron laser ablated by 40 mJ/pulse at the sample into a condensing $Ar/N_2=100/1$ stream for 6.5 h.

TABLE I. Isotopic product absorptions (cm^{-1}) for the boron–nitrogen reaction in solid argon.

$^{11}B+^{14}N_2$	$^{11}B+^{15}N_2$	$^{10}B+^{14}N_2$	$^{10}B+^{15}N_2$	Identification
760.3	736.5	765.8	744.3	species *C*, NNBN
882.3	862.3	901.6	882.0	species *A*, cyclic B_2N
929.5	909.6	950.7	930.8	(perturbed *A*)
1484.8	1481.3	1549.4	1545.9	species *D*, BBNN
1736.5	1701.6	1769.2	1735.2	species *B*, linear BNB
1802.0	1782.3	1859.6	1840.6	species *C*, NNBN
1846.4	1838.5	1892.5	1885.4	$(BO)(N_2)$
1854.5	1854.5	1907.7	1907.7	BO
1912.6	1850.3	1913.7	1851.5	species *D*, BBNN
1958.8	1926.0	2004.8	1973.2	species *E*, BNBN
1998.4	1977.4	2068.8	2048.1	species *A*, cyclic B_2N
2091.7	2022.4	2092.1	2022.7	species *C*, NNBN

pulsed laser assisted reaction of B and N atoms, and a natural isotopic spectrum is shown in Fig. 1(b). The latter *A* bands were increased 20% by 254 nm photolysis and were decreased on annealing. The satellite absorptions diminished and the spectrum appeared identical to the spectrum obtained from a sample prepared by ablation of BN.

Further experiments were done with doping to check for possible impurity reactions. Ablated BN vapors codeposited with $Ar/O_2=200/1$ gave the same spectrum as reported in Fig. 1; the observation of only a trace of BO_2 indicates that atomic B is not a major vapor component. A drop of H_2O was placed on the BN target in a sealed container for two weeks, and the spectrum of the ablated vapors contained strong $B(OH)_3$ absorptions that are described elsewhere,[11] in addition to the bands from BN described above. Similar doping with D_2O gave $B(OD)_3$ bands in addition to the same BN evaporation products.

Boron nitride powder was pressed into a KBr disc and the infrared spectrum was recorded; weak 795 and strong 1370 cm^{-1} bands were observed (100 cm^{-1} full width at half maximum) with the latter an order of magnitude stronger. Boron nitride vapor was trapped in excess argon on a sapphire window at 15±2 K for examination of ultraviolet and visible spectra to check for B atoms. The absorption band for boron atoms[12,13] was observed at 208 nm and a weak band with three vibronic peaks was observed at 307.2, 302.5, and 298.2 nm; no other bands were observed from 300 to 1200 nm. The latter vibronic series was not observed with boron as the target.

TABLE II. Isotopic absorptions (cm^{-1}) for the major product of boron nitride ablation and boron–nitrogen reaction in solid argon.

11-15-11	11-14-11	Absorbance	$\nu_{1/2}$[a]	11-14-10	10-14-10	10-15-10
862.3	882.3	(0.40)	1.7	891.1	901.6	882.0
1977.4	1998.3	(0.05)	1.5	2024.5	2068.8	2048.1
3259	3330	(0.08)	2.6	3370	3407	3339
4358	4425	(0.07)	2.4	4488	4555	4493
5444	5506	(0.10)	2.3	5587	5685	5630
5778	5882	(0.54)	5	5935	5972	5887
6074	6123	(0.60)	8	6152	6191	6134

[a] $\nu_{1/2}$ is the full width at half maximum for the 11-14-11 isotopic bands of given absorbance in Fig. 1.

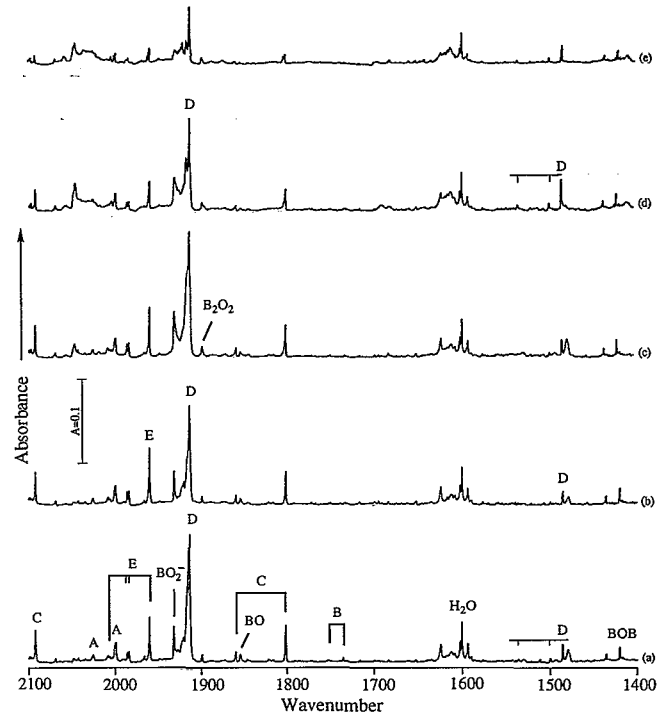

FIG. 2. Infrared spectra in the 2100–1400 cm^{-1} region for natural isotopic boron and nitrogen. (a) Sample codeposited for 6.5 h at 12±1 K; (b) after 254 nm photolysis for 0.5 h; (c) after annealing to 25±2 K; (d) after annealing to 30±2 K; (e) after annealing to 35±2 K.

B. Boron plus nitrogen

Matrix experiments with natural boron atoms evaporated into argon with trace impurity reagents contained a weak 1912.6 cm^{-1} band and a weak 882.3 and 891.1 cm^{-1} doublet.[10] These absorptions were observed with H_2O or D_2O reagents or dilute O_2 but not concentrated O_2 doped samples.[7,10] With ^{11}B atoms only the 1912.6 and 882.3 cm^{-1} bands were observed, but with ^{10}B, weak new 901.6 and 1913.7 cm^{-1} bands were observed. Annealing increased these bands by a factor of 2 to 3. Very weak bands were also observed at 1484, 1736, 1802, 1959, and 2092 cm^{-1} with ^{n}B. In experiments doped with N_2, the above bands increased markedly and provided the basis for the following investigation.

An extensive series of isotopic $B+N_2$ experiments was conducted, and representative spectra are illustrated in Figs. 1(b) and 2(a). After codeposition of natural isotopic boron atoms with 1% N_2 in argon sample, the spectra show weak BO_2 (not illustrated), BOB, BO, $(BO)_2$, and BO_2^- bands.[7] New bands include a strong 1/2 doublet at 891.1 and 882.3 cm^{-1} with an 898 cm^{-1} side band (labeled *A*), a sharp 1484.8 band with a broader satellite at 1479.0 cm^{-1} (labeled *D*), sharp weak 1/2 doublet at 1753.5 and 1736.5 cm^{-1} (labeled *B*), a 1/4 doublet at 1859.6–1802.0 cm^{-1} (labeled *C*), a new band at 1912.6 cm^{-1} (labeled *D*), a 1/4/4/16 quartet at 2004.8, 1985.0, 1983.1, and 1958.7 cm^{-1} (labeled *E*), the 1998.4 cm^{-1} band (labeled *A*), and a new band at 2091.8 cm^{-1} (labeled *C*). Additional weak bands at 769 and 929 cm^{-1} are also listed in Table I. A 30 min 254 nm photolysis increased the strong

A bands by 20% and the *E* quartet by 40%, decreased the two *D* bands by 15% and destroyed the *B* bands leaving other features unchanged as shown in Fig. 2(b). Annealing to 25 K decreased the *A* and *E* bands by 15%, increased the *D* bands by 25% and revealed a shoulder at 1915.0, and left the *C* bands unchanged, Fig. 2(c). Further annealing to 30 K decreased and substantially sharpened the *A* band, increased the sharp *D* site at the expense of the broader site and revealed a 1/4/4/16 quartet at 1549.4, 1535.8, 1499.1, and 1484.8 cm^{-1}; a 1/4 doublet at 2117–2047 cm^{-1} previously identified as molecular BOBO (Ref. 7) also increased on this annealing [Fig. 2(d)]. The final annealing to 40 K decreased all absorptions, left *A* and *D* as the dominant species, and removed the extra bands within the *A* multiplet leaving a sharp 1/8/16 triplet at 901.6/882.3/891.1 cm^{-1}.

The nitrogen concentration in argon was increased from trace impurity levels to 0.2%, 1%, 5%, 25%, and 100% (pure nitrogen matrix). In the 0.2% experiment the aforementioned bands were, of course, weaker. In contrast, annealing to 25 K increased the *A* bands by 15% and further annealing decreased the *A* band by 30%. The two *D* bands showed an increase in the sharper matrix site absorption and a decrease in the broader site band on annealing to 20 and 25 K then the sharp site decreased on annealing to 30 K. The major effect of increasing N_2 concentration on the product population was to increase the yield of species *C* relative to the other products. At 5% N_2 the *C*, *D*, and *A* band absorbances were comparable and at 25% N_2, the *C* bands were three to fourfold more intense. In pure N_2, the *C* bands were an order of magnitude stronger than other product absorptions.[9]

Laser power was varied from 10, to 20, 40, and 60 mJ/pulse at the boron target for experiments with 1% N_2 in argon. One must keep in mind that both photon and boron atom flux depend on laser power. With 10 mJ/pulse no green emission was observed from the condensing sample and the 1913 cm^{-1} band dominated all other product absorptions by factors of 7–9, whereas with 20 and 40 mJ/pulse the 1913 and 882 cm^{-1} product bands were comparable and substantial green emission, indicative of the presence of N atoms,[14] was observed from the condensing sample. The overall product yield increased with laser power, but sample transmission also decreased faster.

One sample was subjected to a filtered photolysis study using 420, 380, and 340 nm long-wavelength pass filters and the full arc including the strong lines near 250 nm. The major effect of this study was a pronounced growth of the *C* bands (25±3%) with 470 nm cutoff radiation which increased to 37% at 380 nm and 41±1% at 340 nm followed by a substantial 40% decrease with the full arc. Both species *D* and *E* showed small gains at 470 and 380 nm but 340 nm photolysis increased *E* and decreased *D* and the full arc further increased *E* at the expense of *D*. In most experiments species *A* bands increased slightly on full arc photolysis.

A complete isotopic substitution study was done for both reagents and spectra in the 2100–1400 cm^{-1} region are compared in Fig. 3 using ^{11}B, ^{10}B, $^{14}N_2$, and $^{15}N_2$ reagent pairs. The boron and nitrogen isotopic absorptions in this region are listed in Table I. Note the large nitrogen isotopic shift for the higher *D* band and the large boron isotopic shifts for the lower *D* band. Likewise the higher and lower *C* bands showed large nitrogen and medium boron isotopic shifts, respectively.

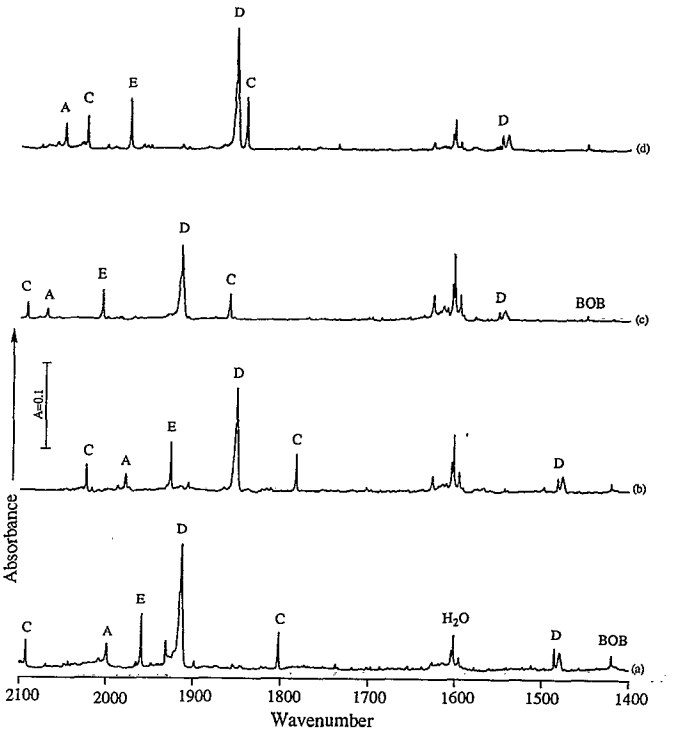

FIG. 3. Infrared spectra in the 2100–1400 cm^{-1} spectral region for isotopic boron and nitrogen samples in argon ($Ar/N_2=100/1$, 40 mJ/pulse at the sample). (a) $^{11}B+^{14}N_2$; (b) $^{11}B+^{15}N_2$; (c) $^{10}B+^{14}N_2$; (d) $^{10}B+^{15}N_2$.

Figures 4 and 5 contrast boron isotopic reactions with the mixed nitrogen isotopic sample containing 48/42/10 ratios of $^{14}N_2/^{14}N^{15}N/^{15}N_2$. In the lower region (Fig. 4) the *A* bands become strong isotopic doublets with site splittings. On annealing to 35 K, minor sites were removed and a sharp 7/3 doublet remained in agreement with the 14/15 isotopic abundance ratio (69/31) for the sample [Figs. 4(a) and 4(c)]. Band positions were identical with $^{14}N_2/^{14}N^{15}N/^{15}N_2$ and $^{14}N_2/^{15}N_2$ reagents. In the upper region (Fig. 5), several mixed isotopic quartets were observed, and these absorptions are listed in Tables III–V. In a $^{14}N_2/^{15}N_2$ experiment with ^{11}B, the 1802.0, 1800.6, 1783.7, and 1782.3 cm^{-1} quartet was observed identical to that from the $^{14}N_2/^{14}N^{15}N/^{15}N_2$ sample showing that two different N_2 molecules provide the N atoms for species *C*. However, the *D* and *E* quartets in Fig. 5(a) become doublets with $^{14}N_2/^{15}N_2$ showing that the N_2 reagent molecule remained intact.

Species *B* exhibited a mixed nitrogen isotopic doublet showing the participation of a single N atom. The lower species *D* band at 1484.8 cm^{-1} showed a small nitrogen isotopic shift to 1481.2 cm^{-1} in the $^{14}N_2/^{15}N_2$ experiment. With the $^{14}N_2/^{14}N^{15}N/^{15}N_2$ sample, new unresolved shoul-

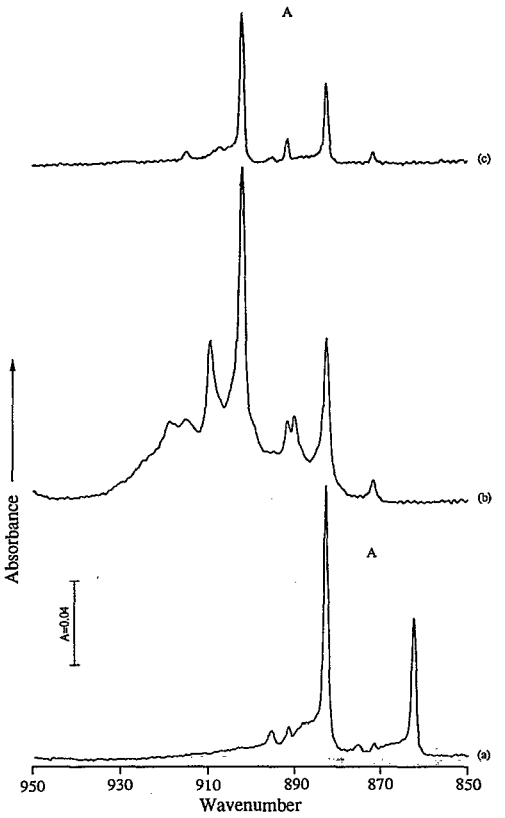

FIG. 4. Infrared spectra of boron atoms codeposited with mixed isotopic nitrogen samples (48% $^{14}N_2$; 42% $^{14}N^{15}N$; 10% $^{15}N_2$) in argon (Ar/N_2 = 100/1) in the 950–850 cm^{-1} region. (a) ^{11}B after annealing to 35±2 K and recooling to 12±1 K; (b) ^{10}B after codeposition at 12±1 K; (c) ^{10}B after annealing to 35±2 K.

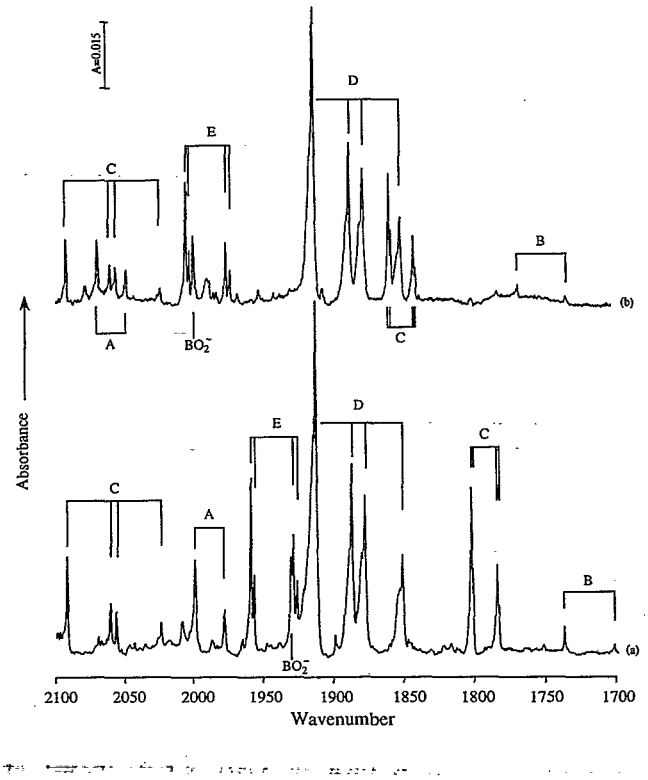

FIG. 5. Infrared spectra of boron atoms codeposited with mixed isotopic nitrogen samples (48% $^{14}N_2$; 42% $^{14}N^{15}N$; 10% $^{15}N_2$) in argon (Ar/N_2 = 100/1) in the 2100–1700 cm^{-1} region after codeposition at 12±1 K: (a) ^{11}B; (b) ^{10}B.

ders appeared at 1484.0 and 1481.9 cm^{-1} showing the minor effect of two inequivalent nitrogen atoms on this vibration.

C. Calculations

Ab initio calculations were performed using the GAUSSIAN 90 program package[15] on the NASA Ames Central Computing Facility Cray Y-MP/8643 and the Computational Chemistry Branch Convex C-210. The standard Pople 6-31G* and Huzinaga–Dunning DZP (double-zeta plus polarization) basis sets were used throughout.[16,17] Harmonic frequencies and double-harmonic IR intensities were obtained as analytical second derivatives of the energy.[18] Although this level of theory is certainly inadequate for quantitative purposes, it should be sufficient for predicting isotopic shift patterns, as was clearly shown to be the case for the comparable C_n clusters.[19] In some cases, frequencies were also computed at the MP2 (second-order Møller–Plesset[20]) level, by numerical differentiation of an analytical gradient.[18] The Hartree–Fock wave functions were always tested for internal stability.[21] The relative stability of different structures and electronic states was computed using QCISD(T) (quadratic configuration interaction[22]), an approximate coupled cluster[23] method that is a very good approximation to full CI even for fairly problematic molecules.[24] Although the basis set used here is too small to compute reliable isomerization energies, it is sufficient to establish which structures are energetically favored and which are not, thus narrowing the scope for the experimental assignments.

IV. DISCUSSION

The new binary boron–nitrogen intermediate species will be identified based on observed and calculated isotopic frequencies and reaction mechanisms will be discussed.

TABLE III. Observed and calculated (cm^{-1}) strongest bond stretching fundamentals in NNBN in solid argon.

Isotope	Observed	Scaled[a] calculated	Observed	Scaled[b] calculated
14-14-11-14	2091.7	2093.1	1802.0	1802.8
14-15-11-14	2055.6	2056.3	1800.6	1802.7
15-14-11-15	2059.8	2060.0	1783.7	1780.6
15-15-11-15	2022.4	2022.4	1782.3	1780.5
14-14-10-14	2092.1	2093.3	1859.6	1858.6
14-15-10-14	2056.1	2056.4	1858.0	1858.5
15-14-10-15	2060.1	2060.2	1842.1	1837.2
15-15-10-15	2022.7	2022.6	1840.6	1837.1

[a]Factor 0.771.
[b]Factor 0.827.

TABLE IV. Observed and calculated (cm^{-1}) isotopic stretching fundamentals for linear BBNN in solid argon.

Isotope	Observed	Scaled[a] calculated	Observed	Scaled[b] calculated
11-11-14-14	1912.6	1912.6	1484.8	1483.8
11-11-14-15	1886.5	1887.4	1481.8	1480.1
11-11-15-14	1877.2	1875.4	1484.0	1483.5
11-11-15-15	1850.3	1849.3	1481.2	1479.9
10-10-14-14	1913.7	1914.6	1549.4	1550.3
10-10-14-15	1887.9	1889.7	1546*br*	1546.2
10-10-15-14	1878.1	1877.2	1549*br*	1550.1
10-10-15-15	1851.6	1851.7	1545.9	1546.1
11-10-14-14	1913	1914.6	1535.8	1535.5
10-11-14-14	1913	1912.7	1499.1	1499.3

[a]Factor 0.919.
[b]Factor 0.939.

A. Species *A*: cyclic B_2N

The strong sharp bands in Table II all show natural boron isotopic triplets with the 1/8/16 relative intensity characteristic of two equivalent boron atoms and sharp 7/3 relative intensity doublets in the 48% $^{14}N_2$, 42% $^{14}N^{15}N$, and 10% $^{15}N_2$ experiments indicative of a single nitrogen atom. Clearly species *A* has the B_2N stoichiometry but is not linear BNB because the strong 882.3 cm^{-1} fundamental is too low[5] and has inappropriate isotopic shifts for linear BNB. In fact, the ^{15}N shift is too large for the harmonic vibration of any reasonable species, which led to the consideration of other molecules such as NNB_2. However, preliminary *ab initio* calculations show that the second N atom contributes to the NB_2 normal coordinate, and the observed mixed nitrogen isotopic doublet pattern is not appropriate for NNB_2. If species *A* is cyclic B_2N, then the 882.3 cm^{-1} vibration must be considerably anharmonic.

This possibility receives substantial support from the five combination bands observed in the 3000–6500 cm^{-1} region that are due to species *A*. Note the marked increase in intensity for the last two "combination bands," which is indicative of vibronic mixing with a low-lying excited electronic state of B_2N. The strong fundamental at 882.3 cm^{-1} is assigned to the antisymmetric B–N stretching fundamental $\nu_3(b_2)$ of cyclic B_2N. The 1998.4 cm^{-1} combination band is the sum of $\nu_1(a_1)$, the symmetric B–N stretching fundamental, and ν_3. The difference 1998-882=1116 cm^{-1} provides a measure of ν_1. A preliminary assignment[25] of the 882.3 and 1998.4 cm^{-1} bands to other species is shown here to be incorrect. Differences between the third, fourth, and fifth bands are 1095 and 1081 cm^{-1}, which are clearly intervals for the ν_1 mode. The second-third band difference of 1332 cm^{-1} is more difficult to explain; this interval is probably 2 quanta of the $\nu_2(a_1)$ B–B stretching mode. The much smaller intervals among the last three bands are not fundamentals of the ground-state B_2N molecule; these intervals must be heavily influenced by the perturbing excited electronic state. The vibronic band at 307.2 nm with 500±20 cm^{-1} spacings is most likely due to B_2N, which is the major species present, although we cannot be certain.

In addition to the linear $^2\Sigma_u^+$ ground state found for BNB in previous work,[5] a potential-energy surface search revealed another stationary point on the doublet surface which corresponds to a $^2B_2$ state. (There is no such stationary point on the UHF/3-21G surface, which was used for the initial geometry searches to save on CPU time.)[5] This situation is similar to that for the isoelectronic C_3^+ cation.[26] The computed frequencies (Table VI) differ rather substantially from those for the linear isomer. Unfortunately, attempts to compute the harmonic force field at a higher level of theory met with failure.

Since the highest σ_u and σ_g orbitals are nearly degenerate, one expects the presence of a low-lying $^2\Sigma_g^+$ state, which is obtained by a single $\sigma_g \rightarrow \sigma_u$ excitation. As seen in Table VI, this electronic transition energy is less than 6000 cm^{-1}, which indicates that the higher overtones of the cyclic B_2N ($^2B_2$ state) vibrations will display significant vibronic interaction effects. The observed combination bands involve ν_3 (b_2) and the symmetric vibrational modes. The failure to observe cyclic B_2N in the $^2B_2$ state by ESR (Ref. 4) is most likely due to differences in production and relaxation of the energized evaporated species.

TABLE V. Observed and calculated (cm^{-1}) strongest isotopic antisymmetric stretching fundamental of linear BNBN in solid argon.

Isotope	Observed	*Ab initio* Calculated	Scaled (0.9062)	Δ
10-14-10-14	2004.8	2213.2	2005.6	−0.8
10-14-11-14	1985.0	2190.2	1984.8	+0.2
11-14-10-14	1983.1	2189.1	1983.8	−0.7
11-14-11-14	1958.7	2160.8	1958.1	+0.6
10-15-10-15	1973.2	2177.7	1973.4	−0.2
11-15-10-15	1954.3	2154.6	1952.5	+1.8
10-15-11-15	1950.0	2153.2	1951.2	−1.2
11-15-11-15	1926.0	2124.0	1924.8	1.2
10-14-10-15	2002.3	2210.4	2003.1	−0.8
10-15-10-14	1976.3	2181.2	1976.6	−0.3
11-14-11-15	1956.5	2158.4	1955.9	+0.6
11-15-11-14	1928.8	2127.0	1927.5	+1.3

B. Species *B*: linear B–N–B

The species *B* band shows isotopic data characteristic of two equivalent *B* atoms and one N atom. The 10/11 boron isotopic ratio 1769.2/1736.5=1.0188 and 14/15 nitrogen isotopic ratio 1736.5/1701.6=1.0205 are near the calculated harmonic values for ν_3 of linear B–N–B, namely 1.0192 and 1.0202, and substantiate the infrared identification of linear BNB.

Unrestricted Hartree–Fock (UHF) *ab initio* calculations using the 6-31G* basis set have predicted an extremely intense ν_3 mode for linear BNB at 2271 cm^{-1}.[5] A scale factor of 0.76 is required to relate the *ab initio* and observed matrix fundamentals. The similar BOB molecule[25] was predicted at 1900 cm^{-1} by UHF/6-31G* calculations, which requires a similar 0.75 scale factor to give the observed 1420 cm^{-1} ν_3 fundamental.[10]

Isotopic ν_3 fundamentals can be used to calculate the valence angle for a C_{2v} molecule as described for the similar BOB molecule.[10] Central isotopic substitution 10-14-10/10-15-10 and 11-14-11/11-15-11 predicts valence angle

lower limits of 151° and 154° and terminal isotopic substitution 10-14-10/11-14-11 and 10-15-10/11-15-11 predicts upper limit cosine values of −1.057 and −1.037 which are, of course, not defined. The average cosine value, where anharmonicity effects are minimized, predicts a valence angle of 165° *with sufficient uncertainty to include a linear molecule.* Interestingly, virtually the same valence angle predictions were calculated from isotopic ν_3 fundamentals for BOB.[10] Unfortunately, frequency accuracy, anharmonicity, (which can be large for linear molecules with low-frequency bending modes), and small matrix effects prevent the exclusion of linear structures for BNB and BOB. In the near linear structural range, isotopic ν_3 predictions of valence angle have a large uncertainty. The best structural conclusion is that isotopic ν_3 fundamentals are in accord with linear structures for BNB and BOB, which is in agreement with the ESR spectrum and theoretical calculations[4,5] for BNB and recent calculations[25,27] for BOB.

C. Species *C*: NNBN

Isotopic splittings for the two strong species C bands at 1802.0 and 2091.7 cm^{-1} identify species *C* as NNBN. First, natural boron experiments reveal a 1/4 doublet at 1859.6/1802.0 cm^{-1}, which characterizes the vibration of one boron atom. The 10/11 boron isotopic ratio 1.0319 and the 14/15 nitrogen isotopic ratio 1.0111 show more boron and less nitrogen involvement than BN diatomic. Mixed nitrogen isotopic experiments reveal a quartet at 1802.0, 1800.6, 1783.7, and 1782.3 cm^{-1}, which shows that this vibration involves primarily one nitrogen atom with a small interaction with a second nitrogen atom. Second, the 2091.7 cm^{-1} band shows a small boron isotopic effect (0.4 cm^{-1}) and a large $^{15}N_2$ shift (69.3 cm^{-1}). The 2091.7, 2059.8, 2055.6, and 2022.4 cm^{-1} quartet pattern demonstrates the involvement of two inequivalent (but almost equivalent) nitrogen atoms, and the 14/15 ratio 1.0343 is slightly below the harmonic 1.0350 value for the N_2 diatomic.

The weak band at 760.3 cm^{-1} is appropriate for the N_2–BN stretching fundamental. The 2092, 1802, and 760 cm^{-1} bands increased together as the N_2 concentration was increased in successive experiments. Furthermore, these bands increased together with near UV irradiation of the sample.

Ab initio calculations (HF/6-31G*) predict the three stretching fundamentals for ground- ($^1\Sigma^+$) state NNBN at 2715, 2180, and 732 cm^{-1}. A scale factor 0.771 relates the calculated isotopic N–N stretching frequencies to the observed values with an average difference of 0.6 cm^{-1}, whereas a scale factor 0.827 is required to fit the calculated isotopic B–N stretching frequencies with an average difference of 2 cm^{-1} (Table III). The calculated value for the N_2–BN mode is, however, too low.

The fundamentals for N_2BN show matrix shifts akin to N_2O. The stretching fundamentals are blue shifted in solid N_2 as compared to solid argon [for N_2O in solid N_2 (2236 and 1291 cm^{-1}) and in solid argon (2219 and 1283 cm^{-1})].[28] The NNBN species absorbs at 2125, 1806, and 750 cm^{-1} in solid N_2 where it is the major product species.[9]

Based on experience with BN_2 and N_3, only linear structures have been considered for NNBN. Of the two possible arrangements, NNBN and NNNB, one normally expects the former to be more stable because of the great strength of the NN and BN bonds and the relatively weakly bound[29] N_3, compared to N_2. Indeed, the NNBN arrangement is by far the preferred one (Table VI). Calculations also show that the $^1\Sigma^+$ ground state is definitely preferred over the $^3\Pi$ state: the latter might be an intermediate in the formation of NNBN from ground-state BN($^3\Pi$) and $N_2(^1\Sigma^+)$. (It was recently demonstrated by extensive multireference calculations that BN has a $^3\Pi$ ground state, even though the $^1\Sigma^+$ state is only 380 cm^{-1} higher in energy.)[30] Test calculations showed that the formation of NNBN($^1\Sigma^+$) from N_2 and BN($^1\Sigma^+$) proceeds with zero activation.

Although the computed isotopic shifts are in good agreement with the experimental ones for the bands assigned to NNBN, the band origins require smaller than normal scale factors. Redoing the frequencies at the MP2 level produced a somewhat nonsensical force field: This is not surprising given the misperformance of MP2 for the N_2 molecule.[31] Additionally, it was observed previously[29] that the 6-31G* basis set is really too small for N–N bonds. Hence, the experimental assignments are consistent with the computed results.

D. Species *D*: BBNN

The strong sharp 1912.6 cm^{-1} band and 1915 cm^{-1} shoulder and the weaker sharp 1484.8 cm^{-1} band with broader 1479.0 cm^{-1} satellite are assigned to BBNN on the basis of isotopic substitution. The sharp 1912.6 cm^{-1} band shows a small (1.1 cm^{-1}) boron isotopic shift and a larger (62.2 cm^{-1}) nitrogen isotopic shift. The 14/15 ratio 1912.5/1850.3 = 1.0336 is just below the harmonic N_2 value. The $^{14}N/^{14}N^{15}N/^{15}N_2$ quartet shows two slightly inequivalent nitrogen atoms in this vibration. The sharp 1484.8 cm^{-1} band shows a small (3.6 cm^{-1}) $^{15}N_2$ shift and a very large (64.6 cm^{-1}) boron isotopic shift. The 10/11 ratio 1549.4/1484.8 = 1.0435 is just below the harmonic B_2 value of 1.0486. The mixed natural boron isotopic 1/4/4/16 quartet at 1549.5, 1535.8, 1499.1, and 1484.8 cm^{-1} indicates the vibration of two inequivalent boron atoms. Hence, the identification of BBNN is substantiated.

In order to be complete, reasons for rejecting the BNN possibility for the 1912.6 cm^{-1} band must be given. Of course, association of the 1484.8 cm^{-1} band, which clearly involves two inequivalent boron atoms is paramount. In addition, UHF calculations predict the N–N stretching fundamental of BNN to be a weak band at 2003 cm^{-1}, which should scale to 1783 cm^{-1}, too low for assignment of the 1912.6 cm^{-1} band. Finally, the strongest fundamental of BNN has been observed at 958 cm^{-1} in nitrogen matrix studies,[9] and this absorption was not observed in argon matrix experiments.

Annealing these samples to 30 K destroyed the broad *D* bands and increased the sharp *D* component. Photolysis

with 470 and 380 nm cutoff filters slightly increased the species *D* bands, subsequent 340 nm cutoff radiation slightly decreased these bands, and final 254 nm radiation substantially decreased species *D* and increased species *E* bands. Species *E* is identified as the more stable BNBN isomer.

Ab initio calculations (HF/6-31G*) predict stretching fundamentals at 2081, 1580, and 831 cm^{-1} for the $^3\Pi$ state of linear BBNN (Table VI). Scale factors of 0.919 and 0.939 are required to relate the calculated and observed N–N and B–B stretching fundamentals, respectively. The lower BB–NN stretching fundamental calculated at 831 cm^{-1} was not observed.

Table IV lists the observed isotopic fundamentals for BBNN and the values from scaled *ab initio* calculations. Note that the average difference between calculated and observed frequencies is 0.8 cm^{-1}. This excellent frequency fit for two fundamentals confirms the identification of linear BBNN.

E. Species *E*: BNBN

The sharp band at 1958.8 cm^{-1} is assigned to linear BNBN on the basis of isotopic substitution. In natural boron isotopic studies a 1/4/4/16 quartet was observed at 2004.8, 1985.0, 1983.1, and 1958.8 cm^{-1} and with $^{14}N_2/^{14}N^{15}N/^{15}N_2$ a 5/2/2/1 quartet was observed at 1958.8, 1956.5, 1928.8, and 1926.0 cm^{-1}. This vibrational mode involves two inequivalent boron atoms and two inequivalent nitrogen atoms. The small separation between the mixed boron isotopic bands at 1985.0 and 1983.1 cm^{-1} shows that the boron atoms are almost equivalent in this motion and, on the other hand, the large separation between mixed nitrogen isotopic bands at 1956.5 and 1928.8 cm^{-1}, shows that the nitrogen atoms clearly are not equivalent as one N atom is heavily involved and the other couples a very small amount. This mode can be described as the antisymmetric B–N–B stretching mode in B–N–B–N. Species *E* shows a steady increase on visible and near UV photolysis and a marked increase with 254 nm radiation at the expense of the less stable BBNN isomer.

Ab initio calculations (HF/6-31G*) predict the most intense mode for linear BNBN ($^3\Pi$) by an order of magnitude to be 2161 cm^{-1} (Table VI). The scale factor 0.9062 relates all of the calculated isotopic fundamentals to the observed values, Table V, with an average difference of 0.8 cm^{-1}, which confirms the observation of linear BNBN.

Electronic structure for B_2N_2 species is much less straightforward than for BN_3. The subject molecule is isoelectronic with C_4, and one expects linear and rhombic structures, the latter having closed-shell singlet ground states and the former having the following low-lying states:

$$^3\Sigma^-,{}^1\Delta,{}^1\Sigma:(5\sigma)^2(6\sigma)^2(7\sigma)^2(1\pi)^4(8\sigma)^2(9\sigma)^2(2\pi)^2,$$

$$^3\Sigma^+:(5\sigma)^2(6\sigma)^2(7\sigma)^2(1\pi)^4(8\sigma)^1(9\sigma)^1(2\pi)^4,$$

$$^3\Pi:(5\sigma)^2(6\sigma)^2(7\sigma)^2(1\pi)^4(8\sigma)^2(9\sigma)^1(2\pi)^3,$$

$$^1\Sigma:(5\sigma)^2(6\sigma)^2(7\sigma)^2(1\pi)^4(8\sigma)^2(9\sigma)^0(2\pi)^4.$$

In C_4, the ground state is $^3\Sigma_g^-$; however, like in BN, the near-degeneracy effects in B_2N_2 are such that $^3\Pi$ states are apparently favored (Table VI), except for the case of BNNB. As to be expected here, the closed-shell $^1\Sigma^+$ states are often essentially biconfigurational, exhibiting a large contribution from an $(8\sigma)\rightarrow(9\sigma)$ double excitation. Under these circumstances, it is to be expected that QCISD(T) overestimates the stability of these states.

Given the high strength of alternating B–N–B bonds[5,25] and the well-known strong N–N bond, as well as the relatively weak B–B bond, one expects the BNBN arrangement to be the most stable one, followed by BNNB and BBNN of comparable stability and, finally, NBBN. As is seen from Table VI, this pattern is largely obeyed.

Given the fairly substantial energy difference between BNBN and BBNN, it is somewhat surprising that the experimental data indicate the presence of BBNN in addition to the more stable BNBN. The explanation for this is probably kinetic: BBNN is readily formed from B_2 and N_2 and there should be a high barrier to rearrangement to BNBN. The fact that the BNBN absorption increases on photolysis at the expense of BBNN points in this direction. Note that, under these circumstances, one might also expect to observe BNNB. The lack of BNNB in these experiments is probably kinetic as well.

For the rhombic B_2N_2 structure of D_{2h} symmetry, two distinct arrangements are possible with either B atoms, or the N atoms, along the shorter diagonal. Apparently (Table VI), the former arrangement is the more stable one. Somewhat surprisingly, it has a triplet state that is predicted to fall below BNBN($^3\Pi$) in energy. The SCF frequencies exhibit one negative eigenvalue; however, this is probably an artifact of the Hartree–Fock approximation as an MP2 frequency calculation yields all positive eigenvalues. More elaborate calculations will be required to determine which structure is actually the lowest in energy. Although rhombic B_2N_2 was not observed here, it was a minor product in similar nitrogen matrix experiments where more of the reactive BN intermediate was formed.[9]

F. Mechanisms

The major pulsed laser evaporated species from solid BN is cyclic B_2N with a smaller quantity of linear BNB. In addition, a low yield of B and N atoms give a trace of the B+N atom reaction products described:

$$\text{BN (solid)} + \text{pulsed laser} \rightarrow B_2N(^2B_2) \text{ and } BNB(^2\Sigma_u^+). \quad (1)$$

The major reaction product of laser evaporated boron and nitrogen with low laser power and minimum radiation is BBNN, which probably arises from the reaction of excited $B_2(^3\Pi)$, made from the B+B reaction and N_2:

$$B(^2P) + B(^2P) + N_2(^1\Sigma_g^+) \rightarrow B_2(^3\Pi) + N_2(^1\Sigma_g^+) \rightarrow BBNN(^3\Pi) \quad (2)$$

TABLE VI. HF/6-31G* geometries and harmonic frequencies, and QCISD(T)/6-31G* total (hartree) and relative (kcal/mol) energies, for various structures of B_2N, B_2N_2, and BN_3. IR intensities for active modes are given in parentheses after the frequencies.

Structure	State	Total energy	Relative energy	Geometry (Å, deg)	Frequencies (cm^{-1}); intensities (km/mol)
BNB	$^2\Sigma_u^+$	−104.009 31	0.0	r_{BN}=1.309	2271(σ_u, 8782), 1245(σ_g), 82(π_u, 5)
	$^2B_2$	−104.006 76	1.6	r_{BN}=1.325, θ_{BNB}=81.5	1608(a_1, 102), 1178(b_2, 388), 643(a_1, 8)
	$^2\Sigma_g^+$	−103.982 10	17.1	r_{BN}=1.292	2224(σ_u, 5153), 1352(σ_g), 440(π_u, 99)
$(BN)_2$ (D_{2h})	$^3B_{2g}$	−158.635 53	0.0	r_{BN}=1.417, θ_{BNB}=68.8	1366(a_g), 1081(a_g), 986(b_{1u}, 50), 962(b_{3g}), 498(b_{3u}, 80), 675i(b_{2u})
BNBN	$^3\Pi$	−158.630 48	3.2	r_{BN}=1.245, r_{NB}=1.362, r_{BN}=1.301	2161(σ, 1045), 1862(σ, 75), 897(σ, 3), 525 and 499(π, 59 and 124), 196 and 191(π, 1 and 0)
$(BN)_2$ (D_{2h})	^1A_g	−158.595 20	25.3	r_{BN}=1.386, θ_{BNB}=65.1	1588(a_g), 1266(b_{1u}, 840), 1178(a_g), 1086(b_{2u}, 233), 715(b_{3u}, 136), 560(b_{3g})
BNNB	$^1\Sigma_g^+$	−158.579 39	35.2	r_{BN}=1.225, r_{NN}=1.288	2332(σ_g), 1683(σ_u, 15267), 1009(σ_g), 584(π_g), 204(π_u, 28)
BNNB	$^3\Sigma_u^+$	−158.556 72	49.5	r_{BN}=1.224, r_{NN}=1.286	2337(σ_g), 2039(σ_u, 55), 1042(σ_g), 464(π_g), 242(π_u, 17)
BBNN	$^3\Pi$	−158.556 29	49.7	r_{BB}=1.504, r_{BN}=1.360, r_{NN}=1.143	2081(σ, 345), 1580(σ, 4), 831(σ, 12), 495 and 366(π, 0 and 1), 226 and 215(π, 1 and 4)
NBBN	$^3\Pi_u$	−158.533 22	64.2	r_{BN}=1.318, r_{BB}=1.590	1767(σ_g), 1458(σ_u, 439), 640(σ_g), 406 and 342(π_g), 185 and 167(π_u, 22 and 20)
$(BN)_2$ (D_{2h})	^1A_g	−158.508 45	79.7	r_{BN}=1.592, θ_{NBN}=46.3	1670(a_g), 908(b_{1u}, 962), 721(a_g), 309(b_{3u}, 17), 197(b_{3g}), 134(b_{2u},9)
NBBN	$^1\Sigma_g^+$	−158.445 22	119.4	r_{BN}=1.255, r_{BB}=1.713	1982(σ_g), 608(σ_u, >100000), 531(σ_g), 380(π_g), 162(π_u, 22)
BNBN	$^1\Sigma^+$	−158.42(48)[a]	(132)	r_{BN}=1.198, r_{NB}=1.437, r_{BN}=1.234	2280(σ, 59), 2135(σ, 0), 784(σ, 35), 537(π, 47), 223(π, 13)
NNBN	$^1\Sigma^+$	−188.524 36	0.0	r_{NN}=1.080, r_{NB}=1.446, r_{BN}=1.227	2715(σ, 210), 2180(σ, 69), 732(σ, 47), 544(π, 4), 185(π, 17)
NNNB	$^1\Sigma^+$	−188.464 53	37.5	r_{NN}=1.095, r_{NN}=1.199, r_{NB}=1.366	2644(σ, 1134), 1786(σ, 1150), 987(σ, 95), 641(π, 34), 172i(π, 0.03)
NNBN	$^3\Pi$	−188.461 20	39.6	r_{NN}=1.162, r_{NB}=1.339, r_{BN}=1.340	2236(σ, 351), 1746(σ, 49), 858(σ, 12), 512 and 339(π, 78 and 35), 221 and 296i(π, 31 and 3)

[a]Unsatisfactory QCISD(T) convergence (see text).

The involvement of an intact N_2 molecule is demonstrated by the observation of only pure isotopic product absorptions in the $^{14}N_2/^{15}N_2$ experiments. This reaction occurs on *deposition* and on *annealing* the cold sample to 20 and 25 K. The $B_2(^3\Pi)$ state is only 3500 cm^{-1} above the ground $^3\Sigma_g^-$ state,[32] and its ready reaction with N_2 is suggested.

With increasing laser power, the green glow of $N(^2D)$ emission appears, providing evidence for the presence of N atoms[14] and cyclic B_2N becomes a major product. The reaction probably goes through BN, although the BN species was not directly detected; excited BN also reacts directly with N_2 to give NNBN, which was a major product. Excited BN is made by irradiation or reaction (3). Recall the growth of NNBN on near ultraviolet photolysis in the region of the allowed $A\,^3\Pi \leftarrow X\,^3\Pi$ absorption of BN;[33] relaxation in the matrix can produce the more reactive intermediate a $^1\Sigma^+$ state. The more stable $BNBN(^3\Pi)$ species is made from rearrangement or photolysis of BBNN, reaction (6). Again the isotopic doublet absorptions with $^{14}N_2/^{15}N_2$ reagent show that BNBN is produced from a single N_2 molecule:

$$B(^2P)+N(^4S)\rightarrow BN(^3\Pi \text{ and } {}^1\Sigma^+), \quad (3)$$

$$B(^2P)+BN(^3\Pi)\rightarrow B_2N(^2B) \text{ and } BNB(^2\Sigma^+), \quad (4)$$

$$N_2(^1\Sigma_g^+)+BN(^1\Sigma^+)\rightarrow NNBN(^1\Sigma^+), \quad (5)$$

$$BBNN(^3\Pi)+h\nu(254\text{ nm})\rightarrow BNBN(^3\Pi). \quad (6)$$

V. CONCLUSIONS

Pulsed laser evaporation of boron atoms into a condensing argon stream doped with N_2 produced new boron–nitrogen species and gave evidence for dissociation of molecular nitrogen into atoms. Reactions of B and N atoms at high dilution in argon favored diboron species and, in contrast, the same experiments done with boron and pure nitrogen produced primarily monoboron species.

At low laser power, the dominant product was BBNN involving an intact N_2 molecule. At higher laser power, dissociation of N_2 by hyperthermal boron atom reactions and/or radiation from the laser produced target emission was evidenced by the intense green glow of $N(^2D)$ atoms. Nitrogen atom reactions involving BN gave NNBN, B_2N, and BNB in addition to BBNN and its rearrangement or photolysis product BNBN.

The major species pulsed laser evaporated from solid BN was the cyclic B_2N radical with a smaller quantity of liner BNB. These species were identified from boron and nitrogen isotopic multiplets and agreement between the observed isotopic frequencies and isotopic frequencies from scaled *ab initio* calculations. This work emphasizes the importance of *ab initio* calculations in the search for new transient molecular species in a complicated binary system such as boron and nitrogen.

ACKNOWLEDGMENTS

We gratefully acknowledge financial support from National Science Foundation Grants CHE 88-20764 and

CHE 91-22556, and helpful discussions and a boron nitride sample from L. B. Knight, Jr. J. M. is a Senior Research Assistant of the National Science Foundation of Belgium (NFWO/FNRS) and acknowledges Fulbright-Hays and NATO travel grants. Part of this work was done while J. M. was a visitor at NASA-Ames Research Center, which provided computer time.

[1] *Gmelins Handbook of Inorganic Chemistry, 8th Ed., Boron Compounds* (Springer, Berlin, 1988), 3rd Suppl., Vol. 3.
[2] S. Becker and H. J. Dietze, Int. J. Mass Spec. Ion Proc. **73**, 157 (1986).
[3] M. D. Morse (private communication).
[4] L. B. Knight, Jr., D. W. Hill, T. J. Kirk, and C. A. Arrington, J. Phys. Chem. **96**, 555 (1992).
[5] J. M. L. Martin, J. P. Francois, and R. Gijbels, J. Chem. Phys. **90**, 6469 (1989).
[6] M. McCluskey and L. Andrews, J. Phys. Chem. **95**, 3545 (1991).
[7] T. R. Burkholder and L. Andrews, J. Chem. Phys. **95**, 8697 (1991).
[8] L. Andrews, T. R. Burkholder, and J. T. Yustein, J. Phys. Chem. (to be published).
[9] P. Hassanzadeh and L. Andrews, J. Phys. Chem. (to be published).
[10] L. Andrews and T. R. Burkholder, J. Phys. Chem. **95**, 8554 (1991).
[11] L. Andrews and T. R. Burkholder, J. Chem. Phys. (to be published).
[12] W. R. K Graham and W. Weltner, J. Chem. Phys. **65**, 1516 (1976).
[13] G. H. Jeong and K. J. Klabunde, J. Am. Chem. Soc. **108**, 7013 (1986).
[14] O. Oehler, D. A. Smith, and K. Dressler, J. Chem. Phys. **66**, 2097 (1977).
[15] M. J. Frisch, M. Head-Gordon, G. W. Trucks, J. B. Foresman, H. B. Schlegel, K. Raghavachari, M. Robb, J. S. Binkley, C. Gonzalez, D. J. Defrees, D. J. Fox, R. A. Whiteside, R. Seeger, C. F. Melius, J. Baker, R. L. Martin, L. R. Kahn, J. J. P. Stewart, S. Topiol, and J. A. Pople, Gaussian 90 Revision (Gaussian, Inc., Pittsburgh, PA, 1990).
[16] W. J. Hehre, R. Ditchfield, and J. A. Pople, J. Chem. Phys. **56**, 2257 (1972); P. C. Hariharan and J. A. Pople, Chem. Phys. Lett. **16**, 217 (1972); Theor. Chim. Acta **28**, 213 (1973).
[17] S. Huzinaga, J. Chem. Phys. **42**, 1293 (1965); T. H. Dunning Jr., *ibid.* **53**, 2823 (1970).
[18] J. A. Pople, R. Krishnan, H. B. Schlegel, and J. S. Binkley, Int. J. Quantum Chem. Symp. **13**, 225 (1979).
[19] J. M. L. Martin, J. P. Francois, and R. Gijbels, J. Chem. Phys. **93**, 8850 (1990).
[20] C. Møller and M. S. Plesset, Phys. Rev. **46**, 618 (1934); J. S. Binkley and J. A. Pople, Int. J. Quantum Chem. **9**, 229 (1975).
[21] R. Seeger and J. A. Pople, J. Chem. Phys. **66**, 3045 (1977).
[22] J. A. Pople, M. Head-Gordon, and K. Raghavachari, J. Chem. Phys. **87**, 5968 (1987).
[23] R. J. Bartlett, J. Phys. Chem. **93**, 1697 (1989).
[24] T. J. Lee, A. P. Rendell, and P. R. Taylor, J. Phys. Chem. **94**, 5463 (1990).
[25] J. M. L. Martin, J. P. Francois, and R. Gijbels, Chem. Phys. Lett. **193**, 243 (1992).
[26] P. R. Taylor, J. M. L. Martin, J. P. Francois, and R. Gijbels, J. Phys. Chem. **95**, 6530 (1991), and references therein.
[27] J. Leszczynsk and J. S. Kwiatkowski, J. Phys. Chem. **96**, 4148 (1992).
[28] D. F. Smith, Jr., J. Overend, R. C. Spiker, Jr., and L. Andrews, Spectrochim. Acta **28A**, 87 (1972).
[29] J. M. L. Martin, J. P. Francois, and R. Gijbels, J. Chem. Phys. **93**, 4485 (1990).
[30] J. M. L. Martin, T. J. Lee, G. E. Scuseria, and P. R. Taylor, J. Chem. Phys. (to be published).
[31] R. F. Hout, Jr., B. A. Levi, and W. J. Hehre, J. Comp. Chem. **3**, 234 (1982).
[32] S. R. Langhoff and C. W. Bauschlicher, J. Chem. Phys. **95**, 5882 (1991).
[33] H. Bredohl, I. Dubois, Y. Houbrechts, and P. Nzohabonayo, J. Mol. Spectrosc. **112**, 430 (1985).